11th World Congress on Structural and Multidisciplinary Optimization
7th - 12th, June 2015, Sydney Australia

Aerothermoelastic Structural Topology Optimisation for a Hypersonic Transport Aircraft Wing

David J. Munk[1], Gareth A. Vio[2], Grant P. Steven[3]

[1] School of AMME, The University of Sydney, NSW, Australia, david.munk@usyd.edu.au
[2] School of AMME, The University of Sydney, NSW, Australia, gareth.vio@usyd.edu.au
[3] School of AMME, The University of Sydney, NSW, Australia, grant.steven@usyd.edu.au

1. Abstract
Aerothermoelasticity plays a vital role in the design of hypersonic aircraft as a strong coupling exists between the aerothermodynamic loads and the structural response. Fluid-thermal-structural interactions are one of the multi-disciplinary problems that must be solved for the design of hypersonic aircraft. Existing optimisation algorithms lack the capability to include these aerothermodynamic coupling effects. This article presents a novel bi-directional evolutionary structural topology optimisation algorithm that includes aerothermoelastic coupling effects. The time-varying temperature distribution is applied through an original formulation, solving for equilibrium of convective, radiative and through thickness conduction at each time step, with a time-marching unsteady conduction solution for time integration. The thermal solution is coupled with a high order aerodynamic solver and the structural finite element model. The results presented in this article show that the coupling between the thermal, structural and aerodynamic forces drive the optimisation of the design and must be taken into consideration to achieve a feasible working structure for the required environment.
2. Keywords: Hypersonic; Aerothermoelastic; Evolutionary; Aircraft.

3. Introduction
Hypersonic flight has been an active area of research for the past six decades, motivated by shorter flight times and reusable launch vehicles for affordable access to space [1]. In a recent review paper, McNamara and Friedmann [2] conclude that accurate modeling of the aerothermodynamics is crucial for the design of hypersonic vehicles. Furthermore the design of the airframe is crucial in order to survive the harsh environment [2]. Current high speed, high enthalpy tunnels are not suitable for the testing of scaled models of hypersonic vehicles [3]. Also, hypersonic aerothermoelastic scaling laws are not available at high Mach numbers [4]. Therefore, the development of accurate computational aerothermodynamic simulation capabilities is important for the design and analysis of hypersonic vehicles.

Aerothermodynamic applications to structural topology optimisation have not yet been considered for lightweight design. Eschenauer and Olhoff [5] and Krog *et al.* [6] both studied the internal design of wing ribs using topology optimisation methods. However, the aerodynamic load was prescribed and therefore not design dependent. Studies that have included aerodynamic loading feedback, to model aerodynamic-structure coupling, in the optimisation are shown in [7, 8]. These studies dealt with steady aerodynamic-structural coupling. Stanford and Beran [9] looked at dynamic aerodynamic-structural coupling. However, none of these studies had a temperature model included in the analysis. Stanford and Beran [10] recently added a thermal model, however a temperature profile is prescribed along the solid-fluid interface, therefore no aero-thermo coupling is present.

This paper extends the previous work by developing a structural topology optimisation algorithm with a strong coupling between the aerodynamics and thermodynamics. The article optimises the wing of a generic hypersonic cruise vehicle in its cruise condition for minimum weight. The importance of the aerothermodynamic coupling on the design of the structure is analysed.

4. Theoretical Analysis
The wing structure used in this article is the LAPCAT A2 [11]. A finite element mesh is generated from a series of node coordinates. The aerothermoelastic module is shown in Fig. 1.

The inertial and elastic modules make up the finite element analysis (Fig. 1 (left)). A strong coupling exits between the aerodynamic and structural modules, however the weak coupling between the thermal and aerodynamic module is ignored [12]. The weak feedback of the structural deformations on the thermal module is included in the analysis.

The inputs and outputs of the different modules are shown in Fig. 1 (right). MATLAB® is used to communicate between the different modules and check for convergence of optimisation.

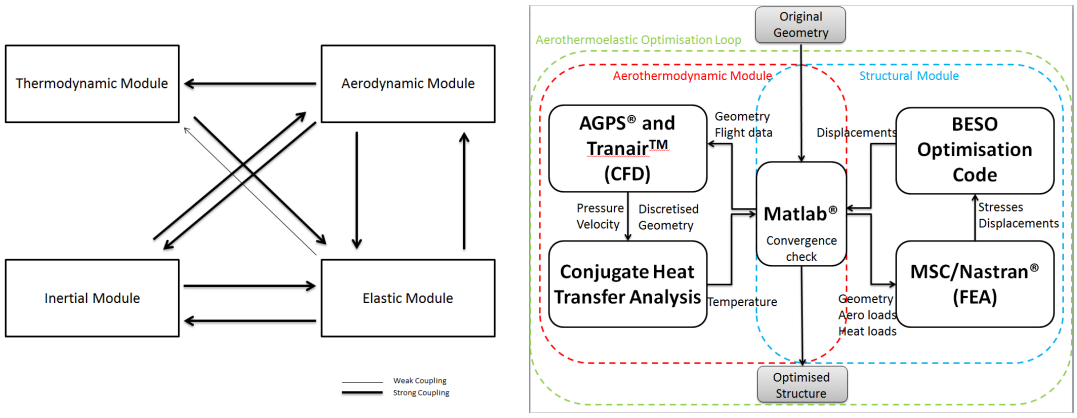

Figure 1: Degree of Coupling for the Aerothermoelastic Domain (left), Optimisation Network for Aerothermoelastic Coupling (right).

4.1. Structural Module

The structural deformation and stresses are calculated by performing a finite element analysis. The finite element software used is MSC/Nastran®. The initial structural model is shown in Fig. 2 (left).

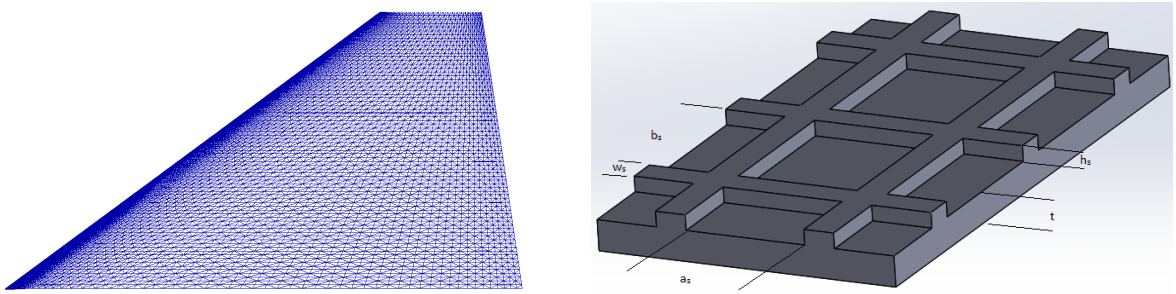

Figure 2: Initial Structural Model (left), Cross-Stiffened Skin (right).

The model uses four node shell elements (Fig. 2 (left)), since aircraft structures are built from metal plates. The initial model begins with all possible combinations of spars, ribs and cross-bars.

4.2. Aerodynamic Module

Two complementary software packages are used in the aerodynamic module, AGPS™ and Tranair®. AGPS™, the Aero Grid and Panelling System, takes the vehicles geometry and generates the grid points for an aerodynamic mesh. AGPS™ efficiently and accurately produces such a mesh, which can be updated from deformations in the structure, such that the structural module can update the aerodynamic module.

AGPS™ produces the input files for the aerodynamic solver Tranair®. The surface and wake meshes are written into a Tranair® input file, specifying the coordinates of each corner point of the mesh. Tranair® solves the non-linear, full potential equation for three-dimensional flow at subsonic, transonic and supersonic Mach numbers [13]. Tranair® uses an adaptive rectangular flow-field grid, which relieves the computational expense of generating a surface fitted flow-field grid for complex geometries by using a rectangular mesh that adapts to the vehicle surface. Tranair® has a boundary layer coupling incorporated into the code. The output of the aerodynamic module is the discretised geometry, used for all the other modules, the pressure loading on the wing, and the boundary layer edge properties, used to calculate the surface temperature in the thermal module.

4.3. Thermal Module

The temperature loading on the wing is determined by solving an equilibrium calculation at the solid-fluid interface. Heat is transferred by convection, due to aerodynamic heating, radiation of the skin to the environment and internal conduction. The solution is then stepped forward in time by solving the unsteady conduction equation.

At the fluid-solid interface the equilibrium condition states that:

$$q_{conv} - q_{rad} = q_{cond} \tag{1}$$

therefore, an expression for the temperature of the skin can be derived. The expression is solved for the wall temperature, T:

$$\sigma\varepsilon T^4 + \left(S_t \rho u C_w + \frac{k_w}{\Delta z}\right) T = S_t \rho u C_{aw} T_{aw} + \sigma\varepsilon T_e^4 + \frac{k_w T_{int}}{\Delta z} \tag{2}$$

where S_t is the Stanton number, C is the specific heat, ρ is the density, k_w is the conductivity coefficient, u is the local velocity at the edge of the boundary layer and Δz is the thickness of the wing skin. Eq. 3 calculates the surface temperature for a given flight condition at every location except in the stagnation region.

4.4. Topology Optimisation Algorithm

Structural failure occurs once a certain stress level is reached in a material, this is a case of under-design. Conversely, over-design is when low stress levels are present in a material. Ideally the stress in every part of a structure is near the same safe level. The evolutionary technique of this work begins with an over designed structure and slowly removes the unused material until a certain stress level is reached in the structure. The optimisation procedure also checks for material that is over-stressed and adds more material in these regions.

The algorithm used in this article is a hard-kill Bi-directional Evolutionary Structural Optimisation (BESO) method [14]. The algorithm is computationally far more efficient, compared to gradient methods, as the hard-killed elements are not involved in the finite element analysis. Furthermore, elements with intermediate densities, such as those found in soft-kill BESO and SIMP algorithms, may cause the global stiffness matrix to become ill-conditioned, particularly for a nonlinear structure. For these reasons the hard-kill BESO method is preferable, particularly for complex three-dimensional structures.

4.4.1. Sensitivity Number and Filter Schemes

When a continuum structure is discretised the sensitivity numbers can become discontinuous across the element boundaries. This leads to checkerboard patterns in the resulting topologies [15]. A secondary issue in topology optimisation is mesh dependency, this is when different topologies are obtained when using different finite element meshes. To overcome such problems nodal sensitivity numbers are defined by averaging the element sensitivity numbers as follows:

$$\alpha_j^n = \sum_{i=1}^{M} w_i \alpha_i^e \tag{3}$$

where M denotes the total number of elements connected to the j^{th} node. α_i^e is the element sensitivity number of the i^{th} element, for a fully stressed design the element sensitivities are defined as:

$$\alpha_i^e = \sigma_i^{vm} \tag{4}$$

w_i is the weight factor of the i^{th} element, defined by:

$$w_i = \frac{1}{M-1}\left(1 - \frac{r_{ij}}{\sum_{i=1}^{M} r_{ij}}\right) \tag{5}$$

where r_{ij} is the distance between the centre of the i^{th} element and the j^{th} node. The nodal sensitivity numbers are then converted into smoothed elemental sensitivity numbers. This is performed by a filter scheme that projects the nodal sensitivity numbers to the design domain. The filter has a length scale r_{min} that does not change with mesh refinement. The purpose of the scale parameter, r_{min}, is to identify the nodes that will influence the sensitivity of the i^{th} element. Where r_{min} must be large enough such that the sub-domain, Ω_i, covers more than one element. Nodes inside the sub-domain Ω_i contribute to the computation of the improved sensitivity number of the i^{th} element as:

$$\alpha_i = \frac{\sum_{j=1}^{K} w(r_{ij}) \alpha_j^n}{\sum_{j=1}^{K} w(r_{ij})} \tag{6}$$

where K is the total number of nodes in the sub-domain Ω_i, $w(r_{ij})$ is the linear weight factor defined as:

$$w(r_{ij}) = r_{min} - r_{ij} \qquad (j = 1,2,\ldots,K) \tag{7}$$

The filter scheme smoothes the sensitivity numbers in the whole design domain. Therefore, the sensitivity numbers for void elements are automatically obtained. Void elements may have high sensitivity numbers due to high sensitivity numbers of solid elements within the sub-domain Ω_i. Therefore, void elements may be turned into solid elements in the next iterations.

This filter scheme is similar to the mesh-independency filter used by Sigmund and Petersson [16], except that node sensitivities are used in Eq. 10 instead of element sensitivities.

With ESO/BESO methods the sensitivity numbers of solid and void elements are based on discrete design variables of element presence (1) and absence (0). This results in convergence difficulties for the objective function and hence topology. Large oscillations are often observed in the evolution history of the objective function. Huang and Xie [17] found that by averaging the sensitivity number with its historical information is an effective way to solve this problem. The simple averaging scheme is given by:

$$\alpha_i = \frac{\alpha_i^k + \alpha_i^{k-1}}{2} \tag{8}$$

where k is the current iteration number. Therefore, the updated sensitivity number includes the whole history of the sensitivity information in the previous iterations.

4.4.2. Ensuring Connectivity

Aircraft structures usually consist of thin shell structures where the outer surface or skin of the shell is usually supported by longitudinal stiffening members and transverse frames to enable it to resist bending, compressive and torsional loads. The internal structure is a continuous frame structure, such that if the skin were removed the remaining structure would not fall apart. Such structures are known as semi-monocoque. Therefore, to ensure such a structure is output by the optimisation algorithm of this article a original connectivity filter has been developed. The connectivity filter ensures that all internal elements are connected. This is done by passing the internal solid elements through a filter that checks all nodes connected to the solid element are connected to another internal solid element.

4.4.3. Panel Buckling

Another consideration of the optimisation process is panel buckling, a common failure mode for high speed aircraft. Nonuniform stress distributions may result in panel buckling, while still having stress levels below the failure point. To prevent panel buckling a technique employed in the NASA developed structural sizing program HyperSizer® [18] is used for the optimisation of the skin.

The critical buckling stress for a plate is calculated by:

$$\sigma_{cr} = \frac{k\pi^2 E}{12(1-\nu^2)} \left(\frac{t}{b}\right)^2 \tag{9}$$

where $k = 4$ for simply supported panels, E is the modulus of elasticity of the plate, ν is the Poisson's ratio, t is the thickness and b is the characteristic length of the plate. The margin of safety of the panel can be calculated by:

$$MS_{buckling} = 1 - \frac{\sigma_{applied}}{\sigma_{cr}} \tag{10}$$

where $\sigma_{applied}$ is the applied buckling stress. For panels with a $MS_{buckling} < 0$ the thickness of the panel is increased. Cross-stiffened panels, see Fig. 2 (right), are used to model the skin of the wing. To reduce the computational space of the optimisiation a smearing technique is employed to model the skin and stringers [19]. The smearing technique is employed by updating the thickness of the shells by:

$$t_e = t + h_s w_s \left(\frac{1}{a_s} + \frac{1}{b_s}\right) - \frac{h_s w_s^2}{a_s b_s} \tag{11}$$

where t is the thickness of the skin, t_s is the thickness of the stringers, w_s and h_s are the width and height of the stringers respectively and a_s and b_s are the spacing of the stringers in the chordwise and spanwise direction.

5. Results and Discussion

The LAPCAT A2 wing is optimised for its cruise condition. The aircraft is flying at Mach 5 with a 1° angle of attack, at an altitude of 25*km*. Due to the brevity of this article only preliminary results are presented, further results will be shown in the presentation.

5. 1. Aerothermoelastic Coupling

The aerothermoelastic module couples the aerodynamic, thermal and structural module to determine the aerodynamic pressure and heating on the wing (see Section 4). The initial pressure and heat loading on the wing is given in Fig. 3.

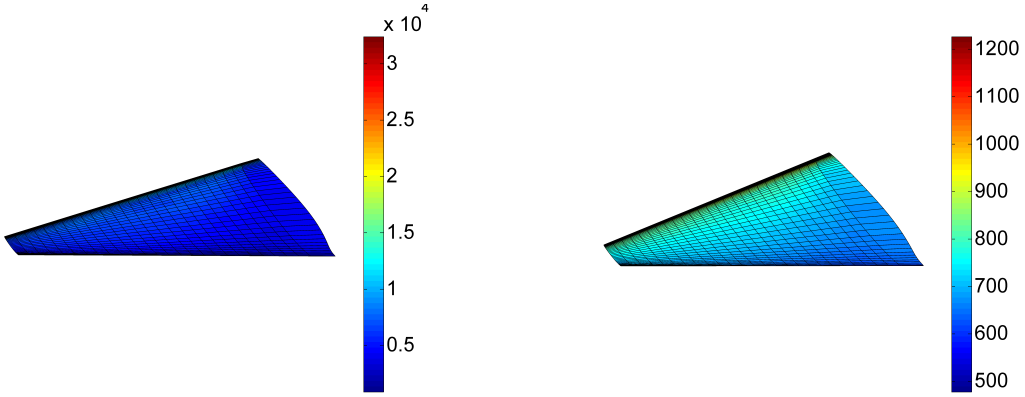

Figure 3: Initial Pressure Loading (left), Initial Thermal Loading (right).

5. 2. Optimisation

The internal structure of the A2 wing has been optimised for the load case defined in Section 5.1. The wing skin is kept unchanged, having a span varying thickness of 6*mm* at the root and 3*mm* at the tip. The internal structure has a constant thickness of 3*mm*. The initial and final stress distribution can be seen in Fig. 4.

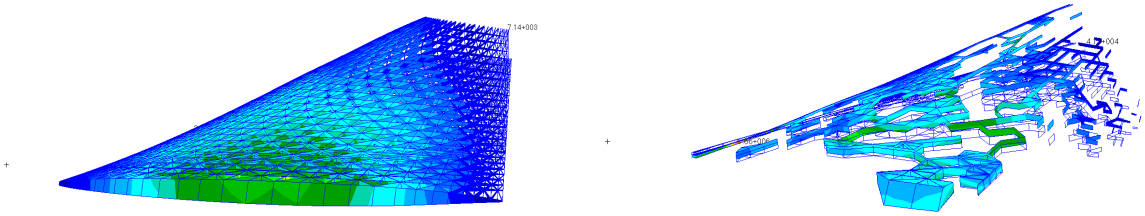

Figure 4: Initial Stress Distribution (left), Final Stress Distribution (right).

The final topology has kept the majority of its structure at the leading edge, since this coincides with the maximum temperature and therefore the region where the material is at its weakest. Furhtermore, due to the low aspect ratio of the A2 wing large bending stresses at the root are not present. Therefore the wing is twisted, along the spanwise axis, causing torsion.

6. Conclusion

A novel bi-directional evolutionary optimisation technique with aerothermoelastic coupling has been demonstrated. The strong coupling between the aerodynamic and structural modules and the aerodynamic and thermal modules has been included. The aerodynamic loading is determined using Tranair®. The thermal loading is calculated by a novel conjugate method, with an unsteady conduction solver for time integration.

The optimisation algorithm was able to satisfy the weight constraint of 20*tons*, without exceeding material limits or causing skin buckling. It was found that the deflections of the wing alter the loadcase significantly, indicating that there is a strong coupling present.

The optimisation algorithm allows multiple preliminary designs to be considered with the aerothermoelastic coupling present. This allows preliminary designs to be considered that have been optimised for a more realistic hypersonic environment.

References

[1] A. A. Rodriguez, J. J. Dickeson, O. Cifdaloz, A. Kelkar, J. M. Vogel, and D. Soloway. Modeling and control of scramjet-powered hypersonic vehicles: Challenges, trends and tradeoffs. *AIAA Guidance, Navigation and Control Conference and Exhibit, AIAA Paper 2008-6793*, 2008.

[2] J. J. McNamara and P. P. Friedmann. Aeroelastic and aerothermoelastic analysis of hypersonic vehicles: Current states and future trends. *AIAA Journal*, 2007.

[3] N. Lamorte and P. P. Friedmann. Hypersonic aeroelastic and aerothermoelastic studies using computational fluid dynamics. *AIAA Journal*, 52:2062–2078, 2014.

[4] J. Dugundji and J. M. Calligeros. Similarity laws for aerothermoelastic testing. *Journal of the Aerospace Sciences*, 29:935–950, 1962.

[5] H. A. Eschenauer and N. Olhoff. Topology optimization of continuum structures: A review. *American Society of Mechanical Engineers*, 2001.

[6] L. Krog, A. Tucker, M. Kemp, and R. Boyd. Topology optimisation of aircraft wing box ribs. *Altair Technology Conference*, 2004.

[7] K. Maute and G. W. Reich. Integrated multidisciplinary topology optimisation approach to adaptive wing design. *Journal of Aircraft*, 43:253–263, 2006.

[8] B. Stanford and P. Ifju. Aeroelastic topology optimization of membrane structures for micro air vehicles. *Struc. Multidisc. Optim.*, 38:301–316, 2009.

[9] B. Stanford and P. Beran. Optimal structural topology of a plate-like wing for subsonic aeroelastic stability. *Journal of Aircraft*, 48:1193–1203, 2011.

[10] B. Stanford and P. Beran. Aerothermoelastic topology optimization with flutter and buckling metrics. *Structural and Multidisciplinary Optimization*, 48:149–171, 2013.

[11] R. Varvill and A. Bond. Lapcat ii a2 vehicle structure design specification. Technical report, Long Term Advanced Propulsion Concepts and Technologies II, 2008.

[12] M. Rodgers. Aerothermoelasticity. *AeroSpace Engineering*, pages 34–43, 1958.

[13] Boeing Company. *TRANAIR User's Manual*. Boeing Company, 2009.

[14] X. Huang and Y. M. Xie. *Evolutionary Topology Optimization of Continuum Structures*. John Wiley and Sons, 2010.

[15] C. S. Jog and R. B. Harber. Stability of finite element models for distributed-parameter optimization and topology design. *Comput. Meth. Appl. Mech. Engng.*, 130:1951–1965, 1996.

[16] O. Sigmund and J. Petersson. Numerical instabilities in topology optimization: a survey on procedures dealing with checkerboards, mesh-dependecies and local minima. *Struct. Optim.*, 16:68–75, 1998.

[17] X. Huang and Y. M. Xie. Convergent and mesh-independent solutions for the bidirectional evolutionary structural optimization method. *Finite Elem. and Des.*, 43:1039–1049, 2007.

[18] M. D. Ardema. Structural sizing for buckling critical body structure of advanced aircraft. *J. Aircraft*, 40:1208–1211, 2003.

[19] Y. Luan, M. Ohlrich, and F. Jacobsen. Smearing technique for vibration analysis of simply supported cross-stiffened and doubly curved thin rectangular shells. *J. Acoust. Soc. Am.*, 129:707–716, 2011.